INL/CON-22-67932-Revision-0

HI-STORM Overpack and MPC-32 Thermal-Hydraulic Model with MOOSE Framework

November 2022

Changing the World's Energy Future

Sinan Okyay, Fande Kong, Peter German, Guillaume Louis Giudicelli, Alexander D Lindsay, David Alan Reger, Elia Merzari, Victor Coppo Leite

Idaho National Laboratory

INL is a U.S. Department of Energy National Laboratory operated by Battelle Energy Alliance, LLC

INL/CON-22-67932-Revision-0

HI-STORM Overpack and MPC-32 Thermal-Hydraulic Model with MOOSE Framework

Sinan Okyay, Fande Kong, Peter German, Guillaume Louis Giudicelli, Alexander D Lindsay, David Alan Reger, Elia Merzari, Victor Coppo Leite

November 2022

Idaho National Laboratory
Idaho Falls, Idaho 83415

http://www.inl.gov

Prepared for the
U.S. Department of Energy
Under DOE Idaho Operations Office
Contract DE-AC07-05ID14517

HI-STORM Overpack and MPC-32 Thermal-Hydraulic Model with MOOSE Framework

Sinan Okyay,* Elia Merzari,* Fande Kong,† David Reger,* Peter German,† Victor Coppo Leite,* Guillaume Giudicelli,† and Alexander D. Lindsay†

*The Pennsylvania State University, State College, PA, sko5200@psu.edu , emerzari@anl.gov
† Idaho National Laboratory, Idaho Falls, ID, fande.kong@inl.gov

doi.org/10.13182/T127-39572

INTRODUCTION

Nuclear power is a significant source of electricity in the United States, but the average age of U.S. nuclear power plants is around 40 years old. Safe management of spent nuclear fuel (SNF) is a key aspect of the back-end of the nuclear fuel cycle. Spent fuel dry storage systems are now a popular and effective solution in this regard, given the absence of a final disposal system. The spent fuel cask system (i.e., dry cask method) provides a feasible solution for maintaining spent fuel for ~60 years leading up to final disposal [1].

Dry cask storage has many attractive characteristics. It fulfills Nuclear Regulatory Commission (NRC) safety requirements, while also providing modularity and flexibility to contractors [2].

The HI-STORM overpack and MPC-32 canister are the primary components of the HI-STORM 100 dry cask storage system. They remove heat from the system via natural circulation, with no human intervention required. This characteristic provides passive heat removal and low maintenance features in dry cask storage systems. To develop a thermal model for a dry cask storage system, the physics behind the system should be clearly defined. There are two natural circulation loops in the system; circulation of helium cools down the nuclear assemblies in the MPC, while circulation of air cools down the MPC walls. The flow patterns for both these systems are shown in Figure 1, taken from the Final Safety Analysis Report (FSAR) file for the HI-STORM 100 system [3].

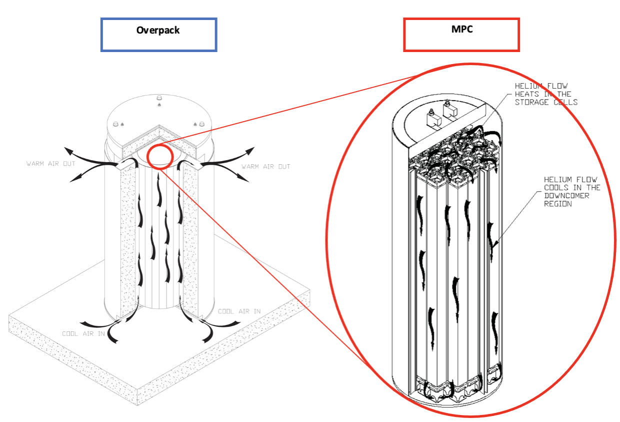

Fig. 1. Flow patterns in the dry cask storage system, retrieved from [3]

This work aims to develop a thermal model of the MPC-32 canister and HI-STORM overpack, using the Multiphysics Object-Oriented Simulation Environment (MOOSE). MOOSE is an open-source framework developed by Idaho National Laboratory (INL) [4] for multiscale, multiphysics simulations. In this study, we investigate and demonstrate MOOSE's thermal-hydraulics modeling capabilities, including the modelling of natural circulation, heat transfer, and porous flow.

METHODS

We used a systematic approach to simulate this system. Overall, three (3) numerical models are discussed, in order of complexity. This modeling strategy is sketched out in Figure 2.

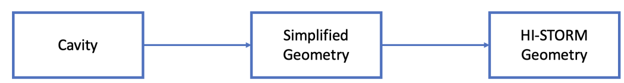

Fig. 2. Modeling strategy

The first model focuses on validation and verification of the results. A differentially heated cavity was chosen as the test case. Cavity systems are often used to measure the validity and performance of computational fluid dynamics (CFD) codes that include natural convection. Its simplicity and the experimental data available make the cavity system a good candidate for measuring system characteristics. To ensure the validity of the cavity model results, they will be compared with those collected from the other studies [5].

We then developed a second geometry: a simplified one similar to that used in the thermal model for the HI-STORM overpack system. This model provides a means of gradually building up to the HI-STORM geometry by starting with a simpler 2-D geometry that is easier to mesh.

The final step focuses on developing a model consistent with the actual HI-STORM system. We performed a series of sensitivity studies on the domain size and mesh density. Further information on the numerical models and solving methods are provided in the next section.

Governing Equations

The simulation of the HI-STORM system can be divided into three sections: the natural circulation of air, the solid interface between the two fluid domains, and the natural circulation of helium. Each section has its own set of governing equations, as described in the next section.

HI-STORM Overpack - Natural Circulation of Air

The motion of fluids in the continuum limit is dictated by conservation laws. The behavior of any fluid can be determined via the mass, momentum, and energy balance equations. The conservation of mass can be expressed as [6]:

$$\frac{\partial \rho}{\partial t} + \nabla \cdot (\rho u) = 0, \tag{1}$$

where ρ is the fluid density and u represents the fluid velocity. In natural convection problems, it is often convenient to use the Boussinesq approximation. This approximation assumes that the fluid density changes linearly with sufficiently small temperature differences in the system. Density variations are then neglected in the Navier-Stokes equations, but accounted for in the body force gravity term. The Boussinesq approximation can be expressed as:

$$\rho = \rho_0 - \beta\rho_0\Delta T, \tag{2}$$

where the β in the equation represents the thermal expansion coefficient of the system. The time-dependent density term is also neglected in Equation (1). The buoyancy-driven flows can be characterized by the Rayleigh number (Ra), a dimensionless number that represents the ratio of the time scale due to thermal diffusion and the time scale due to convection. When the Rayleigh number increases, the system becomes more unstable and eventually transitions to turbulence [5]. The Rayleigh number is the product of the Grashof and Prandtl numbers:

$$Ra = Gr \times Pr = \frac{g\beta\Delta T L^3}{\nu^2} \times \frac{\nu}{\alpha} = \frac{g\beta\Delta T L^3}{\nu\alpha}, \tag{3}$$

where L is the characteristic length of the system. The final form of the conservation equations—with the non-dimensional numbers and Boussinesq approximation used in the air-circulation section—is as follows [7]:

$$\nabla \cdot (\mathbf{u}) = 0 \tag{4}$$

$$\frac{\partial \mathbf{u}}{\partial t} + (\mathbf{u} \cdot \nabla)\mathbf{u} = -\nabla(P) + \frac{Pr}{\sqrt{Ra}}\nabla^2\mathbf{u} - PrT\frac{\mathbf{g}}{|\,\mathbf{g}\,|} \tag{5}$$

$$\frac{\partial T}{\partial t} + \mathbf{u} \cdot \nabla T = \frac{1}{\sqrt{Ra}}\nabla^2 T. \tag{6}$$

MPC-32 - Natural Circulation of Helium

The flow characteristics of the MPC differ from those of the HI-STORM overpack, due to the presence of the fuel assemblies. This region may be treated as a porous medium thanks to the presence of the assemblies in the flow. Heat generation from the assemblies must also be considered. Several new dimensionless parameters may be introduced for porous flow:

$$\begin{aligned} Da = K/L^2, \alpha = hL^2/\varepsilon\kappa_f \\ \gamma = \kappa_s/\kappa_f, \phi = (1-\varepsilon)/\varepsilon\gamma \\ \Gamma = \alpha_s/\alpha_f, \end{aligned} \tag{7}$$

where α_s and α_f are the thermal diffusivities of solid and fluid (these differ from α, which represents the heat transfer coefficient for between phases), and K represents the permeability of the porous medium.

The final form of the conservation equations for porous systems with the Boussinesq approximation and Darcy-Forchheimer friction model used for the MPC helium circulation section is written as follows[8]:

$$\nabla \cdot \mathbf{u} = 0 \tag{8}$$

$$\frac{1}{\varepsilon}\frac{\partial \mathbf{u}}{\partial T} + \frac{1}{\varepsilon^2}(\mathbf{u} \cdot \nabla)\mathbf{u} = -\nabla P + Pr(-\frac{\mathbf{u}}{Da} + \nabla^2\mathbf{u} + RaT \cdot k) \tag{9}$$

$$\frac{\partial T_f}{\partial t} + \frac{1}{\varepsilon}(\mathbf{u} \cdot \nabla)T_f = \Delta T_f + \alpha(T_s - T_f) \tag{10}$$

$$\Gamma\frac{\partial T_s}{\partial t} = \Delta T_s + \frac{\alpha}{\phi}(T_f - T_s). \tag{11}$$

MPC-32 Wall - Interface between the Natural Circulation Loops

The interface between the natural circulation loops is the MPC wall, which is made of a solid material. Since there is no fluid in the interface, the heat conduction equation will be solved. Neither is there any heat generation on the interface.

$$\rho_s C_s \frac{\partial T}{\partial t} = \nabla k_s \nabla T_s \tag{12}$$

Geometry, Mesh, & Solver

To construct and mesh the geometries explained in Figure 2, MOOSE internal modules [4] and the GMSH code[9] were used. The MOOSE modules were used to create the geometry and mesh for the square cavity.

The simplified cask geometry and HI-STORM geometry were constructed and meshed using GMSH. GMSH is an open-source 3-D finite element grid generator that contains a CAD engine to construct the required geometries. It is a fast, user-friendly tool for building desired geometries and meshes [9]. Usage of GMSH will demonstrate MOOSE's capability to integrate with other codes.

To solve the equations described above, we used MOOSE's Navier-Stokes and Heat Transfer modules. The Navier-Stokes module can solve the compressible and incompressible Navier-Stokes (INS) equations via numerical techniques such as Petrov-Galerkin, discontinuous Galerkin, and the finite volume method (FVM). In this study, we demonstrate the solution of the INS equations by using FVM for porous [10] and non-porous media [11]. For each numerical model, the boundary conditions of the equations are provided in the next section.

NUMERICAL MODELS

This section examines the results of 2-D and 3-D simulations of the HI-STORM system.

Cavity

The cavity problem is a standard case that was used to validate and verify the results of the solver. To validate the results of the solver, we constructed isotherms and streamlines to make comparison with literature.

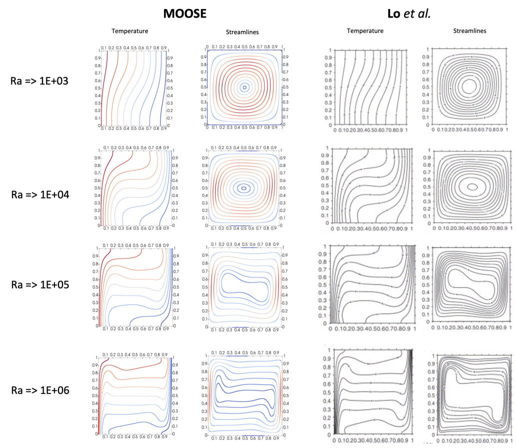

Fig. 3. Cavity comparison.

2-D HI-STORM Geometry (RZ)

The dimensions for the 2-D HI-STORM geometry were taken from the FSAR file [3]. To determine the dimensions of the domain used to represent the ambient air outside the canister (the cold walls in Figure 4), a sensitivity analysis was performed. The geometry in the model shows a sizable dimensional difference when comparing the small vertical channel of HI-STORM Overpack and the cold walls. Thus, in this step, a multi-block meshing strategy is preferred for creating the mesh inside the HI-STORM geometry. A mesh sensitivity analysis was performed to optimize the cost/performance balance in the model.

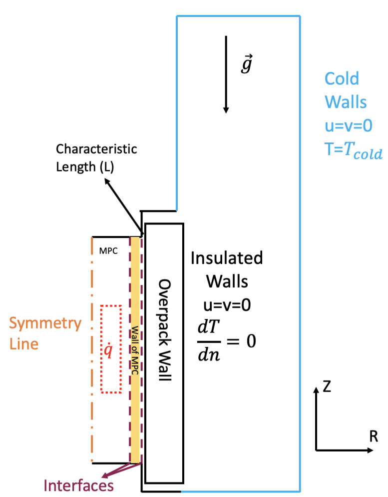

Fig. 4. 2-D sketch of the HI-STORM geometry

The solver settings for the HI-STORM case are presented in Table III.

Mesh Sensitivity

To analyze how the element number of the mesh affects the results, a mesh sensitivity analysis was performed. In this analysis, the geometry was meshed a total of five times, using different numbers of elements. These five cases were run using the same Rayleigh number, and the average flux on the interface between the air channel and MPC wall was calculated. The average heat flux on the interface converged after the third case, indicating that the HI-STORM geometry needs at least 20,000 more elements to become sufficiently resolved.

TABLE I. HI-STORM Case Setup

Name	Value
Solver	Newton
Coordinate System	R-Z
Time Scheme	Transient
Time Step	0.5
Absolute Tolerance	1E-06
Relative Tolerance	1E-06
Velocity Interpolation Method	RC
Advection Interpolation Method	UPWIND

TABLE II. Mesh Convergence Study

MESH CONVERGENCE STUDY		
Case #	**# Elements**	**Interface Flux**
1	5000	-8.91E-05
2	10000	-9.98E-05
3	20000	-1.04E-04
4	40000	-1.08E-04
5	80000	-1.06E-04

Simulation Results

The simulation was run for the geometry shown in Figure 4, and the results, visualized using Paraview [12], are pictured in Figure 5. The preliminary results for the 2-D system are seen in the figure below. Temperature contour and streamlines were produced for the given geometry. The results were produced in a low-power case (approximately 15 kW). The velocity was not fully developed in this case, since natural circulation loops require longer times to reach a steady state. The general behaviour of the circulations is consistent with expectations and with the other studies. The fully developed velocity case will include a circulation flow at the outlet, due to the high momentum of the air escaping the HI-STORM overpack channel. Also, this high-velocity air exhibits a tendency to stick to the cold walls in the system.

3-D HI-STORM Geometry (1/4 Symmetry)

The same model specifications given in Figure 4 and III were used, this time with the properties adjusted for a 3-D simulation. The 3-D simulation was conducted with 1/4 symmetry to lower the computational cost. The results produced for realistic heat sources from each assembly from the previous study. The total power of the cask was around 15 kW. The temperature contour of the system for preliminary result is given in Figure 6. As expected, the heat pattern in the MPC slightly differs from the 2-D R-Z simulation, since we have included additional geometric details in the geometry. At around 450 K, the hottest part of the system is found inside the MPC.

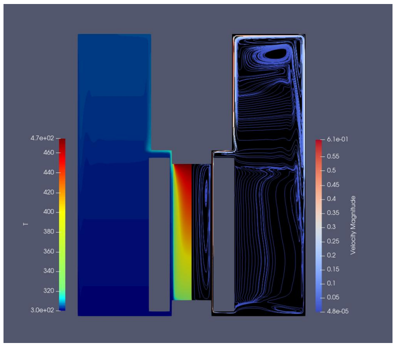

Fig. 5. 2-D (RZ) simulation results, showing velocity (m/s) at right and temperature (K) at left distributions

The temperature distribution and values are consistent with the literature [7].

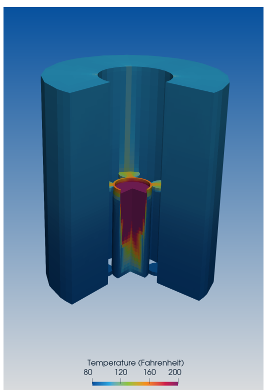

Fig. 6. HI-STORM 3-D temperature contour.

The maximum temperature in the system is compared with available literature. The difference with the previous numerical study is lower than 10% for the same power distribution and geometry. We note that significant differences are expected as the models differ greatly in complexity. In particular the present studies employs a simplified turbulence model. In fact, mixing length turbulence models can only provide tentative answers in complex buoyancy driven flows and the results presented here should be considered only preliminary. Nonetheless the result demonstrate the capability of MOOSE to represent the system with a reasonable degree of accuracy: future work will be dedicated to improve the physical models.

TABLE III. Temperature Comparison

Name	**Value**	**Difference**
Okyay et al.	455 K	**8.8%**
Wu et al.	420 K	

CONCLUSIONS

This study demonstrates the thermal-hydraulic capabilities of the MOOSE framework when applied to dry cask problems. Such problems include natural circulation, heat transfer, and porous flows.The following accomplishments were achieved in this study:

- A reliable solution strategy is built for dry cask problems.
- We validated the MOOSE solver for a prototypical cavity case .
- The thermal-hydraulic models for the MPC-32 and HI-STORM overpack are demonstrated.

REFERENCES

1. D. SHIN, U. JEONG, and S. J. KIM, "CFD Analysis on the Passive Heat Removal by Helium and Air in the Canister of Spent Fuel Dry Storage System," .
2. M. ANGELUCCI, L. E. HERRANZ, and S. PACI, "Thermal analysis of HI-STORM 100S dry cask with the MELCOR code," *Journal of Physics: Conference Series*, **1868**, *1*, 012001 (apr 2021).
3. HOLTEC-INTERNATIONAL, "Holtec International Final Safety Analysis Report for the HI-STORM 100 Cask System," (2016).
4. C. J. PERMANN, D. R. GASTON, D. ANDRŠ, R. W. CARLSEN, F. KONG, A. D. LINDSAY, J. M. MILLER, J. W. PETERSON, A. E. SLAUGHTER, R. H. STOGNER, and R. C. MARTINEAU, "MOOSE: Enabling massively parallel multiphysics simulation," *SoftwareX*, **11**, 100430 (2020).
5. D. LO, D. YOUNG, and C. TSAI, "High resolution of 2D natural convection in a cavity by the DQ method," *Journal of Computational and Applied Mathematics*, **203**, *1*, 219–236 (2007).
6. R. PURAGLIESI, "Numerical investigation of particle-laden thermally driven turbulent flows in enclosure," p. 209 (2010).
7. L. E. HERRANZ, J. PENALVA, and F. FERIA, "CFD analysis of a cask for spent fuel dry storage: Model fundamentals and sensitivity studies," *Annals of Nuclear Energy*, **76**, 54–62 (2015).
8. F. HABBACHI, F. S. OUESLATI, R. BENNACER, and E. AFIF, "Simulation of heat transfer and fluid flow in 3D porous media in non-equilibrium," in "2015 World Symposium on Mechatronics Engineering Applied Physics (WSMEAP)," (2015), pp. 1–12.
9. C. GEUZAINE and J.-F. REMACLE, "Gmsh: A 3-D finite element mesh generator with built-in pre- and post-processing facilities," *International Journal for Numerical Methods in Engineering*, **79**, *11*, 1309–1331 (2009).
10. P. B. R. C. J. O. D. G. M. D. A. A.-J. A. J. N. GUILLAUME GIUDICELLI, ALEXANDER LINDSAY, "Coupled Multiphysics Transient Simulations of the MK1-FHR reactor Using the Finite Volume Capabilities of the MOOSE Framework," in "Mathematics and Computation for Nuclear Science and Engineering," American Nuclear Society (2021).
11. R. F. J. L. GUILLAUME L. GIUDICELLI, ALEXANDER D. LINDSAY, "NEAMS-TH-CRAB," Tech. Rep. INL/EXT-21-62895, Idaho National Laboratory (2021).
12. J. P. AHRENS, B. GEVECI, and C. C. LAW, "ParaView: An End-User Tool for Large-Data Visualization," in "The Visualization Handbook," (2005).